

Article

Electrical Conductivities of Narrow-Bandgap Polymers with Two Types of π -Conjugated Post-Crosslinking

Hao-xuan Guo ^{*}, Hiroshi Takahara, Yusuke Imai and Hiroyuki Aota ^{*}

Department of Chemistry and Materials Engineering, Kansai University, Suita 564-8680, Osaka, Japan; takaharahiroshi895@gmail.com (H.T.); imaiyusuke.425752@gmail.com (Y.I.)

^{*} Correspondence: hx-guo@kansai-u.ac.jp (H.-x.G.); aota@kansai-u.ac.jp (H.A.); Tel.: +81-06-6368-0831 (H.-x.G.)

Abstract: Bandgap energy is one of the most important properties for developing electronic devices because of its influence on the electrical conductivity of substances. Many methods have been developed to control bandgap, one of which is the realization of conducting polymers using narrow-bandgap polymers; however, the preparation of these polymers is complex. In this study, water-soluble, narrow-bandgap polymers with reactive groups were prepared by the addition-condensation reaction of pyrrole (Pyr), benzaldehyde-2-sulfonic acid sodium salt (BS), and aldehyde-containing reactive groups (aldehyde and pyridine) for post-crosslinking. Two types of reactions, aldehyde with *p*-phenylenediamine and pyridine with 1,2-dibromoethylene, were carried out for the π -conjugated post-crosslinking between polymers. The polymers were characterized by proton nuclear magnetic resonance (¹H-NMR), thermogravimetric/differential thermal analysis (TG/DTA), UltraViolet-Visible-Near InfraRed spectroscopy (UV-Vis-NIR), and other analyses. The bandgaps of the polymers, calculated from their absorption, were less than 0.5 eV. Post-crosslinking prevents resolubility and develops electron-conducting routes between the polymer chains for π -conjugated systems. Moreover, the post-crosslinked polymers maintain their narrow bandgaps. The electrical conductivities of the as-prepared polymers were two orders of magnitude higher than those before the crosslinking.

Keywords: π -conjugated polymer; narrow-bandgap polymer; post-crosslinking



Citation: Guo, H.-x.; Takahara, H.; Imai, Y.; Aota, H. Electrical Conductivities of Narrow-Bandgap Polymers with Two Types of π -Conjugated Post-Crosslinking. *Polymers* **2022**, *14*, 2472. <https://doi.org/10.3390/polym14122472>

Academic Editors: Lukasz Klapiszewski and Beata Podkošcielna

Received: 19 May 2022

Accepted: 15 June 2022

Published: 17 June 2022

Publisher's Note: MDPI stays neutral with regard to jurisdictional claims in published maps and institutional affiliations.



Copyright: © 2022 by the authors. Licensee MDPI, Basel, Switzerland. This article is an open access article distributed under the terms and conditions of the Creative Commons Attribution (CC BY) license (<https://creativecommons.org/licenses/by/4.0/>).

1. Introduction

π -Conjugated polymers have received a lot of attention because of their versatility in optical and electronic devices such as organic electroluminescent diodes [1–4], solar cells [5–11], sensors [12–16], and solid electrolyte capacitors [17–21]. Conventional π -conjugated polymers having various donors and acceptors groups, can generate intramolecular charge transfer by the photoexcitation, can control their absorption to match the solar spectrum, and can be used in the solid-state to achieve high charge carrier mobilities [6–11]. In contrast, π -conjugated polymers with doping generate charge carriers (holes and electrons) in the polymer chain and become conductive polymers [22]. The process of doping can introduce a new level between the valence and conduction bands to decrease the bandgap energy (E_g), which allows for an increased mobility of charge carriers between the different energy levels. Sufficiently narrow bandgaps can give rise to high electrical conductivities even in pristine materials. In other words, E_g is one of the most important properties for developing electronic devices because of its influence on the electrical conductivity of substances.

Many methods have been developed to control bandgap [23–26], one of which is the realization of conducting polymers using narrow bandgap polymers [27–40]. However, the preparation of narrow-bandgap polymers ($E_g < 1.0$ eV) [41,42] is complex. Previously, we synthesized water-soluble, narrow-bandgap polymers with $E_g < 0.19$ eV, tuneable in the range 0.3–1.1 eV in aqueous solutions [43,44]. However, their electrical conductivities

were low because of the negligible amount of charge carriers in undoped polymers and the inability of charge carriers conducting between the polymer chains. Recently, we used a post-crosslinking reaction (ester crosslinking) to reduce the distance between the polymer chains, which led to increased electrical conductivity [45]. To further increase their electrical conductivity, we focused on π -conjugated post-crosslinking between the polymer chains, which can provide electron conducting routes between them [46–48]. On the other hand, solubility control is an important parameter in the preparation of electronic devices using polymers. The stability of soluble polymers thin films in some electronic devices that use electrolyte solutions is poor owing to their resolubility. Post-crosslinking can address this issue by preventing resolubility of the polymer thin films [49–51]. Herein, we report the synthesis of water-soluble narrow-bandgap polymers with reactive groups for post-crosslinking by the addition-condensation of pyrrole, sodium salt of benzaldehyde-2-sulfonic acid, and aldehydes containing reactive groups (aldehyde and pyridine). The post-crosslinking step increased the electrical conductivities of the as-prepared polymers by two orders of magnitude, and their resolubility was prevented.

2. Experimental Section

2.1. Materials

Benzaldehyde-2-sulfonic acid sodium salt (BS), terephthalaldehyde mono (diethyl acetal) (TMDA), *p*-phenylenediamine, and 1,2-dibromoethylene were purchased from Tokyo Chemical Industry (Tokyo, Japan). Pyrrole (Pyr), 4-pyridinecarboxaldehyde (pyridineA) and *p*-toluenesulfonic acid monohydrate (*p*-TS) were purchased from FUJIFILM Wako Pure Chemical Corporation (Osaka, Japan). The Pyr monomer was purified via distillation prior to its use.

2.2. Measurements

The UV-Vis-NIR spectra were measured on a JASCO V-670 spectrophotometer, and proton (400 MHz) NMR spectra were recorded on a JEOL ECZ-400S spectrometer. The thermogravimetric/differential thermal analysis (TG/DTA) spectra were measured using a differential thermogravimetric analyzer (Thermo plus TG-DTA 8120, Rigaku, Tokyo, Japan). The sample was scanned from 25 °C to 400 °C with a heating rate of 10 °C/min under air.

For the reduced viscosity (η_{sp}/C) measurement, samples were dissolved in phosphate buffer (4.0 g/L sample solution) and measurements were carried out on a viscometer (Ubbelohde-type) at 30 °C. The molecular weights (M_w) of the polymers were calculated using the Mark–Houwink–Sakurada Equation (1):

$$\eta_{sp}/C = kM_w^\alpha \quad (1)$$

where the constants k (1.16×10^{-5}) and α (0.894) were approximated from the η_{sp}/C and M_w values determined via ultracentrifugal analysis [43].

The E_g was calculated using Equation (2):

$$(\alpha h\nu)^2 = (\text{const}) (h\nu - E_g) \quad (2)$$

Here, α is the absorption coefficient.

The electrical resistances of pressed samples prepared by compressing polymer powder (0.02 g) with a hydraulic press were measured by a four-probe method with a Lorester (MCP-T410, Mitsubishi, Tokyo, Japan). The electrical conductivity of the samples was calculated using Equations (3) and (4):

$$\rho_V = R \times RCF \times t \quad (3)$$

$$\sigma = 1/\rho_V \quad (4)$$

where ρ_V is the volume resistivity (Ω cm), R is resistance (Ω), RCF is resistivity correction factor, t is thickness (cm), and σ is conductivity (S/cm) [45].

2.3. Polymer Synthesis

2.3.1. π -Conjugated Polymers Having Reactive Groups

The non-conjugated polymer **P2** having an acetal group was prepared by reacting a solution of *p*-TS (0.032 g, 0.17 mmol) in DMF (1.0 mL) with another solution of Pyr (0.335 g, 5.0 mmol) and BS (1.041 g, 5.0 mmol) in DMF (5.0 mL) at 10 °C. The mixed solution was stored in the dark. After 24 h, a solution of TMDA (0.104 g, 0.50 mmol) and Pyr (0.034 g, 0.50 mmol) in DMF (2.0 mL) was added to the reaction mixture for 6 h. An aqueous solution of sodium carbonate (5 wt%, 3.2 mL) was added to stop the reaction. Isopropyl alcohol (80 mL) was then added to the reaction mixture. The resulting precipitate, **P2**, was purified by serial reprecipitations, twice from DMF/isopropyl alcohol (8 mL/80 mL), and twice from water/isopropyl alcohol (6 mL/80 mL). The **P2** was finally extracted via freeze-drying (1.296 g).

The π -conjugated polymer, **P4** (with the aldehyde group) was prepared by mixing a solution of DDQ (0.353 g, 1.5 mmol) dissolved in DMF: water (9:1, 6 mL) with a solution of **P2** (0.50 g) in DMF (2.5 mL) at 30 °C. After 6 h, toluene (80 mL) was added to the reaction mixture. Here, the acetal group in the polymer converts to an aldehyde group. The resulting precipitate was purified by a series of reprecipitations from DMF/toluene (8 mL/80 mL) four times, and subsequently from DMF/isopropyl alcohol (8 mL/80 mL), and water/isopropyl alcohol (6 mL/80 mL). The polymer **P4** was finally extracted via freeze-drying (0.461 g).

The polymer **P3** having a pyridyl group (1.011 g) was prepared in a manner similar to that for preparation of **P2**. For the preparation of the π -conjugated polymer, **P5** (having a pyridyl group) was prepared by reacting a solution of chloranil (0.670 g, 2.7 mmol) dissolved in DMF (14 mL), with another solution of **P3** (0.70 g) dissolved in DMF (4.0 mL) at 30 °C. After 6 h, toluene (80 mL) was added to the reaction mixture. The resulting precipitate was purified by serial reprecipitations similar to **P4**. The polymer **P5** was finally extracted via freeze-drying (0.663 g).

2.3.2. Two Types of π -Conjugated Post-Crosslinking Reactions

Type A: Imine type.

P6 was prepared as follows: *p*-TS (0.20 g, 1.0 mmol) was added to a solution of **P4** (with the aldehyde group; 0.20 g) and *p*-phenylenediamine (0.20 g, 1.8 mmol) in DMF (3 mL). The resulting mixture was stirred at 100 °C. After 24 h, the insoluble fraction was separated by suction filtration and washed with water and methanol. **P6** was obtained via vacuum drying (0.088 g).

Type B: Quaternized pyridine type.

P7 was prepared as follows: 1,2-dibromoethylene (0.71 g, 3.8 mmol) was added to a solution of **P5** (having a pyridyl group; 0.30 g) in DMF (3 mL). The resulting mixture was stirred at 100 °C. After 48 h, the insoluble fraction was separated by suction filtration and washed with water and methanol. **P7** was obtained by vacuum drying (0.104 g).

3. Results and Discussion

3.1. Polymerization

The preparation of the polymers is shown in Scheme 1. The addition–condensation polymerization of Pyr with aldehyde monomers BS, TMDA, or pyridine was performed in DMF at 10 °C to obtain the non-conjugated polymers (**P2**, **P3**). **P2** and **P3** were then oxidized to π -conjugated polymers (**P4**, **P5**). Incidentally, the TMDA in **P2** reacted with the oxidant to give an aldehyde via acetal hydrolysis (TMDA). **P2–P5** were soluble in water, methanol, and DMF, and insoluble in isopropyl alcohol, acetonitrile, THF, acetone, chloroform, and hexane. The reduced viscosities and molecular weights of the polymers are summarized in Table 1. The reduced viscosities of **P4** and **P5** are greater than those of **P2** and **P3** because π -conjugation makes the polymer chain rigid. Figure 1 shows the ¹H-NMR spectra of the polymers (**P2–P5**). For **P2** and **P3** (the nonconjugated polymers), the peaks at 9–10 and 5.5 ppm are assigned to the Pyr protons (a and b), the peak at 6.5 ppm is assigned

to the proton (c) between Pyr and BS, and the peaks at 7–8 ppm are assigned to the BS protons (d and e). The peaks at 1.3–1.6 ppm are assigned to the protons in the diethyl acetal group (g) of **P2**. The peaks at 8.3–8.5 ppm are assigned to the protons of the pyridine group (g) in **P3**. After the oxidation reaction, peak broadening can be observed from 5.5 to 8.5 ppm. This can be attributed to the conversion to a π -conjugated system, which causes the polymer chain rigid owing to the slow molecular motion. In the case of **P4**, due to acetal (TMDA) hydrolysis by the oxidant, the peaks at 9.6–10.4 ppm (h) corresponding to aldehyde protons appear. However, for **P5**, the pyridine protons (f) are not assigned because of overlapping peaks and broadening peaks. Due to the low number of reactive groups introduced, the TMDA, pyridine, and aldehyde proton signals are relatively weak. To prove that the reactive groups can be introduced into the polymers, a polymer was synthesized by the same synthetic method using 1-pyrenecarboxaldehyde, which can be spectroscopically monitored. The absorption spectrum of this material confirms the introduction of pyrene units into the polymer (Figure S3). Polymers with a large number of reactive groups were also synthesized as described in the Supplementary Materials. Figures S4 and S5 show the $^1\text{H-NMR}$ spectra of polymers with a large number of reactive groups. The TMDA, pyridine, and aldehyde protons are detected at the same ppm (Figure 1).

Table 1. Properties of polymers.

Compound	η_{sp}/C /dL g $^{-1}$	Mw	Eg/eV
P2	0.134	-	-
P3	0.134	-	-
P4	0.226	63,000	0.48
P5	0.197	54,000	0.43
P(carboxyl) [45]	0.139	36,000	0.55
P(hydroxy) [45]	0.082	20,000	0.62

Ref. [45], **P(carboxyl)**: π -conjugated polymer having a carboxyl group; **P(hydroxy)**: π -conjugated polymer having a hydroxy group.

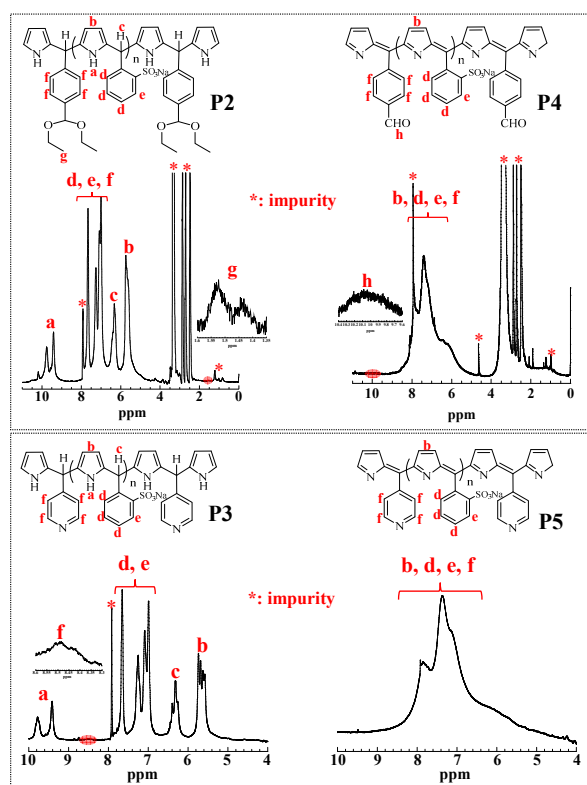
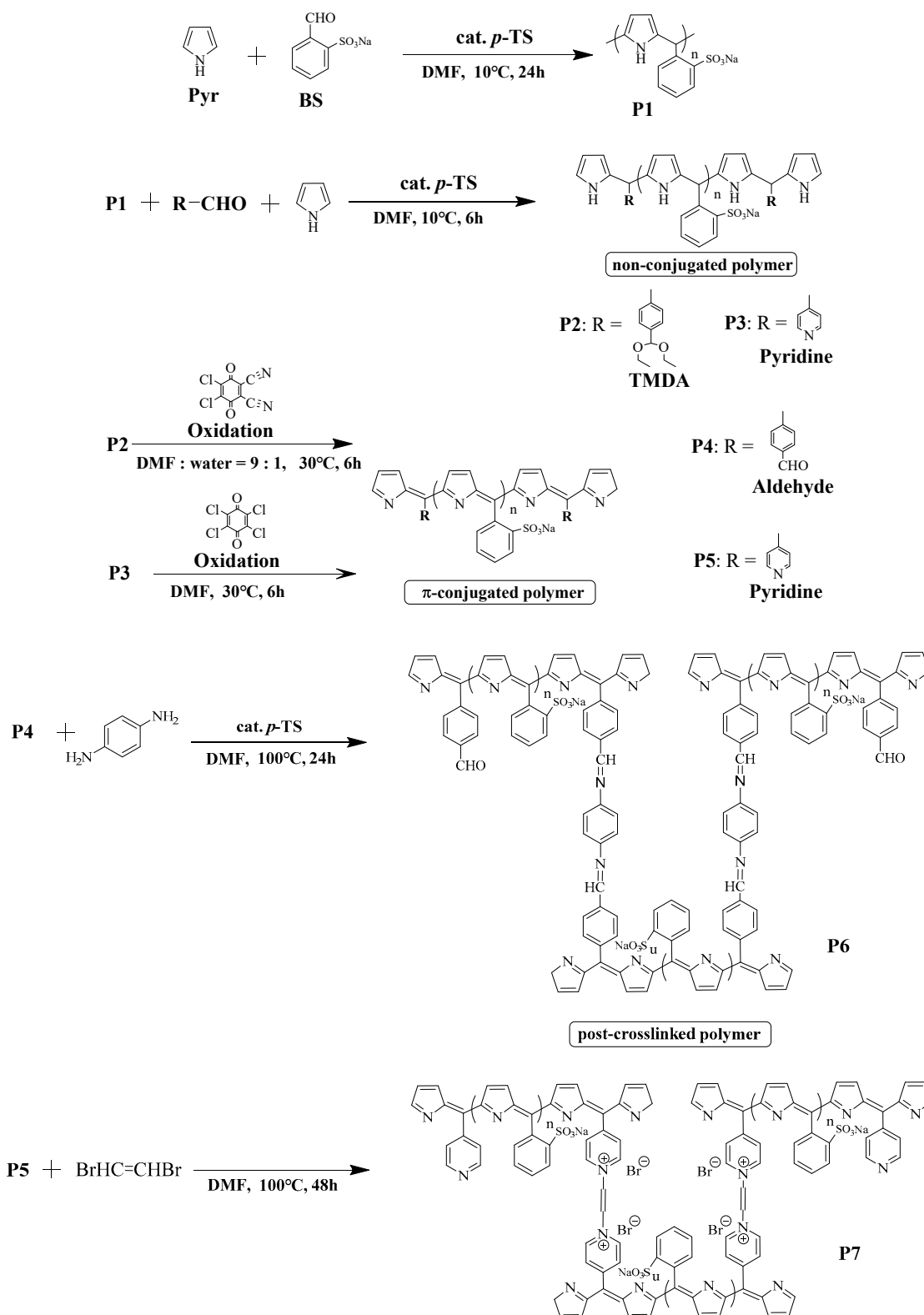


Figure 1. $^1\text{H-NMR}$ spectra of **P2–P5** in $\text{DMSO-}d_6$.



Scheme 1. Synthesis of polymers.

A post-crosslinking reaction was performed as described in Section 2.3. The post-crosslinked polymer **P6** was prepared by imine-crosslinking reaction of **P4** and *p*-phenylenediamine. The post-crosslinked polymer **P7** was prepared by quaternization of pyridine crosslinking reaction of **P5** and 1,2-dibromoethene. **P6** and **P7** were insoluble in almost all the solvents

(water, methanol, ethanol, isopropyl alcohol, acetonitrile, DMF, THF, acetone, chloroform, and hexane). Resolubility of the polymers was prevented by post-crosslinking.

3.2. UV–Vis–NIR Absorption Spectroscopy

Figures 2 and S6 show the UV-Vis-NIR spectra of **P2–P5** dissolved in phosphate buffer (pH 6.9) to prevent self-doping. The longer-wavelength absorptions are due to the π – π^* excitation of the expanded π -conjugation. The bandgaps of the polymers calculated from their absorption are listed in Table 1. The synthesized conjugated polymers were narrow-bandgap polymers ($E_g < 1$ eV) [42].

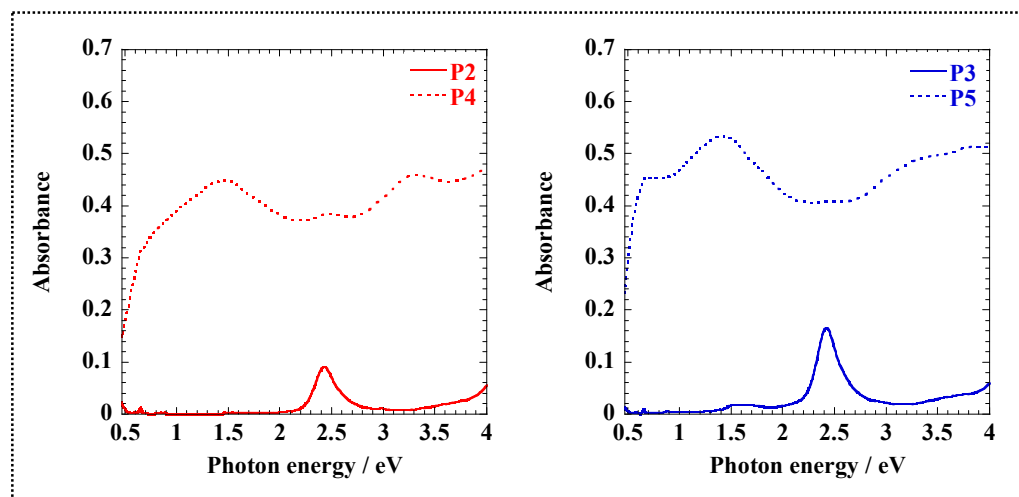


Figure 2. UV-Vis-NIR spectra of **P2–P5** dissolved in phosphate buffer (4.0 g/L).

As the post-crosslinked polymers were insoluble in almost all the solvents, the absorption spectra of the post-crosslinked polymers dissolved in solvent could not be obtained. The diffuse reflection of the polymer powders was measured instead (Figure S7), and the UV-Vis-NIR spectra (Figure 3) of the powdered polymers were obtained using the corresponding diffuse reflection spectra. Compared to the non-conjugated polymers (**P2** and **P3**), the post-crosslinked polymers (**P6** and **P7**) were similar to the π -conjugated polymers (**P4** and **P5**) having a broad absorption band. After the post-crosslinking reaction, **P6** and **P7** maintained their narrow bandgaps.

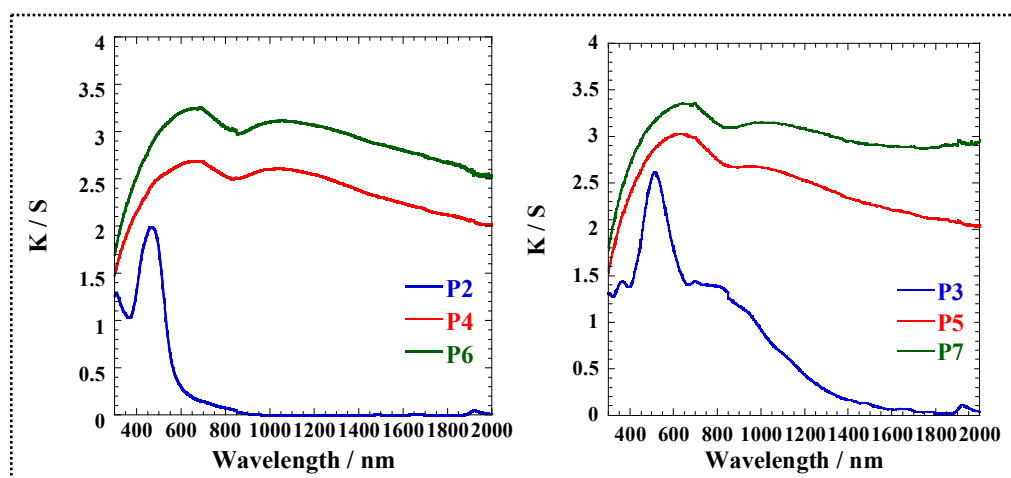


Figure 3. UV-Vis-NIR spectra of **P2–P7** transformed by using diffuse reflection spectra.

3.3. Thermal Stability and Electrical Conductivity Measurements

The thermal stability of the post-crosslinked polymers was investigated via TG/DTA under air. The post-crosslinked polymers **P6** and **P7** recorded an onset decomposition temperature of 300 °C and exhibited a high heat resistance (Figure S8).

A comparison of all the pressed polymer samples (Table 2) reveals that the post-crosslinked polymers show a higher electrical conductivity than those without crosslinking. The conductivity of **P6** and **P7** is 124 and 203 times higher than that of **P4** and **P5**, and significantly higher than the conductivity of our previously studied ester-crosslinked polymers [45]. The improved electrical conductivity occurs due to an improvement in the electron-conducting routes (π -conjugated) between the polymer chains via post-crosslinking (imine-crosslinking and quaternization of pyridine-crosslinking). In addition, **P7** has the highest conductivity, because its charge carriers were generated during the crosslinking reaction between the polymer chains (quaternization of pyridine).

Table 2. Comparison of electrical conductivities of the polymer samples.

Sample	Electrical Conductivity (S cm ⁻¹)
P2	-
P3	-
P4	1.1×10^{-6}
P5	5.9×10^{-6}
P6	1.4×10^{-4}
P7	1.2×10^{-3}
P(carboxyl) [45]	2.3×10^{-7}
P(hydroxy) [45]	1.8×10^{-7}
P(ester) [45]	9.0×10^{-6}

Ref. [45], **P(ester)**: ester-crosslinked polymer.

4. Conclusions

In conclusion, we synthesized novel, reactive, narrow-bandgap polymers with reactive groups, aldehyde and pyridine, via the addition–condensation of Pyr, BS, and TMDA/pyridineA. Imine-crosslinking via the aldehyde group with *p*-phenylenediamine and quaternization of pyridine with 1,2-dibromoethylene were used for the post-crosslinking reaction between the polymer chains. The post-crosslinked polymer was insoluble, maintained a narrow bandgap, and showed a high heat resistance. Post-crosslinking develops π -conjugated, electron-conducting routes between the polymer chains, and charge carriers are generated in the polymer via the quaternization of pyridine. The electrical conductivities of the as-prepared polymers were two orders of magnitude higher than those before the crosslinking. These polymers have great potential in the field of materials science, particularly for the development of novel solid electrolyte capacitors.

Supplementary Materials: The following supporting information can be downloaded at: <https://www.mdpi.com/article/10.3390/polym14122472/s1>, The following are available online at xxx. Figure S1: ¹H-NMR spectrum of **P1** in DMSO-*d*₆, Figure S2: ¹H-NMR spectrum of **Pyr(non)** in DMSO-*d*₆, Figure S3: Absorption spectra of (a) 1-pyrenecarboxaldehyde and pyrene, (b) before and after reaction of **P1** and 1-pyrenecarboxaldehyde dissolved in DMF, Absorption spectrum of (c) polymer containing pyrene dissolved in phosphate buffer (0.04 g/L), Scheme S1: Synthetic routes of polymers, Figure S4: ¹H-NMR spectra of (a) **P(TMDA)** and (b) **P(Aldehyde)** in DMSO-*d*₆, Figure S5: ¹H-NMR spectra of (a) **P(Pyridine)** and (b) **P(Pyridine OX)** in DMSO-*d*₆, Figure S6: UV-Vis-NIR spectra of **P2–P5** dissolved in phosphate buffer (4.0 g/L), Figure S7: Diffuse reflection spectra of the powdered polymers, Figure S8. TGA curves of **P6** and **P7** with a heating rate of 10 °C/min under air, Figure S9. DSC curves of **P6** and **P7** with a heating rate of 10 °C/min under air.

Author Contributions: Conceptualization, H.-x.G. and H.A.; Investigation, H.-x.G., H.T. and Y.I.; Project administration, H.A.; Writing—original draft, H.-x.G. All authors have read and agreed to the published version of the manuscript.

Funding: This is a product of research that was financially supported (in part) by the Kansai University Fund for Supporting Young Scholars, 2018. “Syntheses of amphiphilic polymer and its application to artificial photosynthesis”.

Institutional Review Board Statement: Not applicable.

Informed Consent Statement: Not applicable.

Data Availability Statement: Not applicable.

Acknowledgments: We thank H. Kawasaki (Kansai University) for the measurement of TGA.

Conflicts of Interest: The authors declare no conflict of interest.

References

1. Burroughes, J.H.; Bradley, D.D.C.; Brown, A.R.; Marks, R.N.; Mackay, K.; Friend, R.H.; Burn, P.L.; Holmes, A.B. Light-emitting diodes based on conjugated polymers. *Nature* **1990**, *347*, 539–541. [[CrossRef](#)]
2. Gross, M.; Muller, D.C.; Nothofer, H.-G.; Scherf, U.; Neher, D.; Bräuchle, C.; Meerholz, K. Improving the performance of doped π -conjugated polymers for use in organic light-emitting diodes. *Nature* **2000**, *405*, 661–665. [[CrossRef](#)] [[PubMed](#)]
3. Yang, R.-Q.; Tian, R.-Y.; Yan, J.-G.; Zhang, Y.; Yang, J.; Hou, Q.; Yang, W.; Zhang, C.; Cao, Y. Deep-Red Electroluminescent Polymers: Synthesis and Characterization of New Low-Band-Gap Conjugated Copolymers for Light-Emitting Diodes and Photovoltaic Devices. *Macromolecules* **2005**, *38*, 244–253. [[CrossRef](#)]
4. Kawabata, K.; Saito, M.; Osaka, I.; Takimiya, K. Very Small Bandgap π -Conjugated Polymers with Extended Thienoquinoids. *J. Am. Chem. Soc.* **2016**, *138*, 7725–7732. [[CrossRef](#)]
5. Cheng, Y.-J.; Yang, S.-H.; Hsu, C.-S. Synthesis of conjugated polymers for organic solar cell applications. *Chem. Rev.* **2009**, *109*, 5868–5923. [[CrossRef](#)] [[PubMed](#)]
6. Woo, C.H.; Beaujuge, P.M.; Holcombe, T.W.; Lee, O.P.; Frechet, J.M.J. Incorporation of Furan into Low Band-Gap Polymers for Efficient Solar Cells. *J. Am. Chem. Soc.* **2010**, *132*, 15547–15549. [[CrossRef](#)]
7. Wang, M.; Hu, X.-W.; Liu, P.; Li, W.; Gong, X.; Huang, F.; Cao, Y. Donor-Acceptor Conjugated Polymer Based on Naphtho[1,2-c:5,6-c']bis[1,2,5]thiadiazole for High-Performance Polymer Solar Cells. *J. Am. Chem. Soc.* **2011**, *133*, 9638–9641. [[CrossRef](#)]
8. Cui, C.-H.; Fan, X.; Zang, M.-J.; Zhang, J.; Min, J.; Li, Y.-F. A D-A copolymer of dithienosilole and a new acceptor unit of naphtho[2,3-c]thiophene-4,9-dione for efficient polymer solar cells. *Chem. Commun.* **2011**, *47*, 11345–11347. [[CrossRef](#)]
9. Almeataq, M.S.; Yi, H.; Al-Faifi, S.; Alghamdi, A.A.B.; Iraqi, A.; Scarratt, N.W.; Wang, T.; Lidzey, D.G. Anthracene-based donor-acceptor low band gap polymers for application in solar cells. *Chem. Commun.* **2013**, *49*, 2252–2254. [[CrossRef](#)]
10. Feng, K.; Xu, X.-P.; Li, Z.-j.; Li, Y.; Li, K.; Yu, T.; Peng, Q. Low band gap benzothiophene-thienothiophene copolymers with conjugated alkylthiothiethyl and alkoxy carbonyl cyanovinyl side chains for photovoltaic applications. *Chem. Commun.* **2015**, *51*, 6290–6292. [[CrossRef](#)]
11. Fu, H.; Li, Y.-X.; Yu, J.-W.; Wu, Z.; Fan, Q.-P.; Lin, F.; Woo, H.Y.; Gao, F.; Zhu, Z.-l.; Jen, K.-Y. High Efficiency (15.8%) All-Polymer Solar Cells Enabled by a Regioregular Narrow Bandgap Polymer Acceptor. *J. Am. Chem. Soc.* **2021**, *143*, 2665–2670. [[CrossRef](#)] [[PubMed](#)]
12. Shoji, E.; Freund, M. Potentiometric Saccharide Detection Based on the pKa Changes of Poly (aniline boronic acid). *J. Am. Chem. Soc.* **2002**, *142*, 12486–12493. [[CrossRef](#)] [[PubMed](#)]
13. Herland, A.; Inganäs, O. Conjugated polymers as optical probes for protein interactions and protein conformations. *Macromol. Rapid Commun.* **2007**, *28*, 1703–1713. [[CrossRef](#)]
14. Luo, S.; Ali, E.M.; Tansil, N.C.; Yu, H.; Gao, S.; Kantchev, E.A.B.; Ying, J.Y. Poly(3,4-Ethylenedioxythiophene) (PEDOT) Nanobiointerfaces: Thin, Ultrasoft, and Functionalized PEDOT Films with in Vitro and in Vivo Biocompatibility. *Langmuir* **2008**, *24*, 8071–8077. [[CrossRef](#)]
15. Liu, W.-j.; Pink, M.; Lee, D. Conjugated polymer sensors built on π -extended borasiloxane cages. *J. Am. Chem. Soc.* **2009**, *131*, 8703–8707. [[CrossRef](#)]
16. Taroni, P.J.; Giovanni, S.; Kening, W.; Philip, C.; Manting, Q.; Han, Z.; Pugno, N.M.; Matteo, P.; Natalie, S.S.; Martin, H.; et al. Toward stretchable self-powered sensors based on the thermoelectric response of PEDOT:PSS/polyurethane blends. *Adv. Funct. Mater.* **2018**, *28*, 1704285. [[CrossRef](#)]
17. Kudoh, Y.; Akami, K.; Matsuya, Y. Solid electrolytic capacitor with highly stable conducting polymer as a counter electrode. *Synth. Met.* **1999**, *102*, 973. [[CrossRef](#)]
18. Nogami, K.; Sakamoto, K.; Hayakawa, T.; Kakimoto, M. The effects of hyperbranched poly(siloxysilane)s on conductive polymer aluminum solid electrolytic capacitors. *J. Power Sources* **2007**, *166*, 584–589. [[CrossRef](#)]
19. Shi, Y.; Peng, L.-L.; Ding, Y.; Zhao, Y.; Yu, G.-H. Nanostructured conductive polymers for advanced energy storage. *Chem. Soc. Rev.* **2015**, *44*, 6684–6696. [[CrossRef](#)]

20. Kim, M.; Yoo, J.; Im, H.; Kim, J. The effects of different oxidants on the characteristics of conductive polymer aluminum solid electrolyte capacitors. *J. Power Sources* **2013**, *230*, 1–9. [[CrossRef](#)]
21. Wakabayashi, T.; Katsunuma, M.; Kudo, K.; Okuzaki, H. pH-Tunable High-Performance PEDOT:PSS Aluminum Solid Electrolytic Capacitors. *ACS Appl. Energy Mater.* **2018**, *1*, 2157–2163. [[CrossRef](#)]
22. MacDiarmid, A.G. “Synthetic Metals”: A Novel Role for Organic Polymers (Nobel Lecture). *Angew. Chem. Int. Ed.* **2001**, *40*, 2581–2590. [[CrossRef](#)]
23. Meyers, F.F.; Heeger, A.J.; Bredas, J.L. Fine tuning of the band gap in conjugated polymers via control of block copolymer sequences. *J. Chem. Phys.* **1992**, *97*, 2750–2758. [[CrossRef](#)]
24. Roncali, J. Synthetic Principles for Bandgap Control in Linear δ -Conjugated Systems. *Chem. Rev.* **1997**, *97*, 173–205. [[CrossRef](#)] [[PubMed](#)]
25. Eldo, J.; Ajayaghosh, A. New Low Band Gap Polymers: Control of Optical and Electronic Properties in near Infrared Absorbing π -Conjugated Polysquaraines. *Chem. Mater.* **2002**, *14*, 410–418. [[CrossRef](#)]
26. Cheng, P.; Yang, Y. Narrowing the Band Gap: The Key to High-Performance Organic Photovoltaics. *Acc. Chem. Res.* **2020**, *53*, 1218–1228. [[CrossRef](#)]
27. Kobayashi, M.; Colaneri, N.; Boysel, M.; Wudl, F.; Heeger, A.J. The electronic and electrochemical properties of poly(isothianaphthene). *J. Chem. Phys.* **1985**, *82*, 5717–5723. [[CrossRef](#)]
28. Jenekhe, S.A. A class of narrow-band-gap semiconducting polymers. *Nature* **1986**, *322*, 345–347. [[CrossRef](#)]
29. Becker, R.; Blochl, G.; Braunling, H. Polyheteroarylmethines, Syntheses and Physical Properties. In *Conjugated Polymeric Materials: Opportunities in Electronics, Optoelectronics, and Molecular Electronics*; Springer: Dordrecht, The Netherlands, 1990; Volume 182, pp. 133–139.
30. Braunling, H.; Becker, R.; Blochl, G. Polyarylmethines; Synthesis and Physical Properties. *Synth. Met.* **1991**, *42*, 1539–1547. [[CrossRef](#)]
31. Meyers, F.; Adant, C.; Toussaint, J.M.; Bredas, J.L. AB initio study of the structural, electronic, and nonlinear optical properties of pyrrole derivatives. *Synth. Met.* **1991**, *43*, 3559–3562. [[CrossRef](#)]
32. Toussaint, J.M.; Brédas, J.L. Theoretical analysis of the geometric and electronic structure of small-band-gap polythiophenes: Poly(5,5'-bithiophene methine) and its derivatives. *Macromolecules* **1993**, *26*, 5240–5248. [[CrossRef](#)]
33. Tanaka, S.; Yamashita, Y. Syntheses of narrow band gap heterocyclic copolymers of aromatic-donor and quinonoid-acceptor units. *Synth. Met.* **1995**, *69*, 599–600. [[CrossRef](#)]
34. Akoudad, S.; Roncali, J. Electrogenated poly(thiophenes) with extremely narrow bandgap and high stability under n-doping cycling. *Chem. Commun.* **1998**, *19*, 2081–2082. [[CrossRef](#)]
35. Hong, S.Y. Zero Band-Gap Polymers: Quantum-Chemical Study of Electronic Structures of Degenerate π -Conjugated Systems. *Chem. Mater.* **2000**, *12*, 495–500. [[CrossRef](#)]
36. Mai, C.-K.; Zhou, H.-Q.; Zhang, Y.; Henson, Z.B.; Nguyen, T.-Q.; Heeger, A.J.; Bazan, C.G. Facile Doping of Anionic Narrow-Band-Gap Conjugated Polyelectrolytes During Dialysis. *Angew. Chem. Int. Ed.* **2013**, *52*, 12874–12878. [[CrossRef](#)] [[PubMed](#)]
37. Mai, C.-K.; Schlitz, R.A.; Su, G.M.; Spitzer, D.; Wang, X.-J.; Fronk, S.L.; Cahill, D.G.; Chabiny, M.L.; Bazan, C.G. Side-Chain Effects on the Conductivity, Morphology, and Thermoelectric Properties of Self-Doped Narrow-Band-Gap Conjugated Polyelectrolytes. *J. Am. Chem. Soc.* **2014**, *136*, 13478–13481. [[CrossRef](#)]
38. Poverenov, E.; Zamoshchik, N.; Patra, A.; Ridelman, Y.; Bendikov, M. Unusual Doping of Donor-Acceptor-Type Conjugated Polymers Using Lewis Acids. *J. Am. Chem. Soc.* **2014**, *136*, 5138–5149. [[CrossRef](#)]
39. Mai, C.-K.; Arai, T.; Liu, X.-F.; Fronk, S.L.; Su, G.M.; Segalman, R.A.; Chabiny, M.L.; Bazan, G.C. Electrical properties of doped conjugated polyelectrolytes with modulated density of the ionic functionalities. *Chem. Commun.* **2015**, *51*, 17607–17610. [[CrossRef](#)]
40. Goel, M.; Heinrich, C.D.; Krauss, G.; Thelakkat, M. Principles of Structural Design of Conjugated Polymers Showing Excellent Charge Transport toward Thermoelectrics and Bioelectronics Applications. *Macromol. Rapid Commun.* **2019**, *40*, 1800915. [[CrossRef](#)]
41. Karikomi, M.; Kitamura, C.; Tanaka, S.; Yamashita, Y. New Narrow-Bandgap Polymer Composed of Benzobis(1,2,5-thiadiazole) and Thiophenes. *J. Am. Chem. Soc.* **1995**, *117*, 6791–6792. [[CrossRef](#)]
42. Casado, J.; Ortiz, R.P.; Delgado, M.C.R.; Hernández, V.; Navarrete, J.T.L.; Raimundo, J.-M.; Blanchard, P.; Allain, M.; Roncali, J. Alternated Quinoid/Aromatic Units in Terthiophenes Building Blocks for Electroactive Narrow Band Gap Polymers. Extended Spectroscopic, Solid State, Electrochemical, and Theoretical Study. *J. Phys. Chem. B* **2005**, *109*, 16616–16627. [[CrossRef](#)]
43. Aota, H.; Ishikawa, T.; Amiuchi, Y.; Yano, H.; Kunimoto, T.; Matsumoto, A. Band Gap and Absorption Profile Change by Changing Molecular Weight and Conformation of Water-soluble Narrow-band-gap Polymers. *Chem. Lett.* **2010**, *39*, 1288–1290. [[CrossRef](#)]
44. Aota, H.; Ishikawa, T.; Maki, Y.; Takaya, D.; Ejiri, H.; Amiuchi, Y.; Yano, H.; Kunimoto, T.; Matsumoto, A. Continuous Band Gap Control from 0.3 to 1.1 eV of π -Conjugated Polymers in Aqueous Solution. *Chem. Lett.* **2011**, *40*, 724–725. [[CrossRef](#)]
45. Guo, H.-X.; Ohashi, T.; Imai, Y.; Aota, H. Synthesis of Reactive Water-Soluble Narrow-Band-Gap Polymers for Post-Crosslinking. *Polymers* **2020**, *12*, 313. [[CrossRef](#)] [[PubMed](#)]
46. Rumer, J.W.; McCulloch, I. Organic photovoltaics: Crosslinking for optimal morphology and stability. *Mater. Today* **2015**, *18*, 425–435. [[CrossRef](#)]
47. Lee, H.-J.; Jo, Y.-R.; Kumar, S.; Yoo, S.J.; Kim, J.-G.; Kim, Y.-J.; Kim, B.-J.; Lee, J.-S. Close-Packed Polymer Crystals from Two-Monomer-Connected Precursors. *Nat. Commun.* **2016**, *7*, 12803. [[CrossRef](#)]

48. Chung, Y.; Hyun, K.H.; Kwon, Y. Fabrication of a biofuel cell improved by the π -conjugated electron pathway effect induced from a new enzyme catalyst employing terephthalaldehyde. *Nanoscale* **2016**, *8*, 1161–1168. [[CrossRef](#)]
49. Ochiai, B.; Tomita, I.; Endo, T. Thermal crosslinking of acetylene-containing polymers obtained by radical polymerization of aromatic enynes. *Polymer* **2001**, *42*, 8581–8586. [[CrossRef](#)]
50. Yu, G.-P.; Wang, J.-Y.; Liu, C.; Lin, E.-C.; Jian, X.-G. Soluble and curable poly(phthalazinone ether amide)s with terminal cyano groups and their crosslinking to heat resistant resin. *Polymer* **2009**, *50*, 1700–1708. [[CrossRef](#)]
51. Xu, J.; Wang, J.; Luft, J.C.; Tian, S.-M.; Owens, G.; Pandya, A.A.; Berglund, P.; Pohlhaus, P.; Maynor, B.W.; Smith, J. Rendering Protein-Based Particles Transiently Insoluble for Therapeutic Applications. *J. Am. Chem. Soc.* **2012**, *134*, 8774–8777. [[CrossRef](#)]